Displacement sensing using evanescent tunneling between guided resonances in photonic crystal slabs

Wonjoo Suh,[a] Olav Solgaard, and Shanhui Fan
Department of Electrical Engineering, Stanford University, Stanford, California 94305

Using both analytic theory and first-principles finite-difference time-domain simulations, we introduce a displacement sensing mechanism using photonic crystal slabs coupled in the near-field regime. In this regime, the operating characteristics are completely different from conventional resonant optical sensors, and high sensitivity can be obtained without the use of highly reflecting mirrors. This enables high displacement sensitivity combined with low sensitivity to wavelength and to structural disorders, thereby simplifying operation and fabrication of high-sensitivity displacement sensors. © *2005 American Institute of Physics*. [DOI: 10.1063/1.1999031]

I. INTRODUCTION

Fabry-Perot cavity structures fabricated using micromachining techniques have been widely used for pressure, temperature, and chemical sensing applications.[1–6] The reflectance or transmittance of such cavity structures is a function of both the gap spacing and the wavelength, hence the cavity can be used as a sensor of either parameter.

Specifically, the transmission coefficient t_{total} through a Fabry-Perot cavity [Fig. 1(a)] is dependent upon the relative displacement h between the two reflectors as

$$|t_{total}|^2 = \frac{(1-|r|^2)^2}{(1-|r|^2)^2 + 4|r|^2 \cos^2[\arg(t) - \phi]}. \quad (1)$$

Here $\Phi = (\omega/c) * h$ is the one-way phase shift that the wave acquires as it propagates through the cavity, while r and t are the reflection and transmission coefficients of each reflector. When $\arg(t) - \phi = [m + (1/2)]\pi$, where m is an integer, the cavity becomes resonant with the incident light. In the vicinity of the resonance, the total transmission coefficient exhibits a Lorentzian peak with respect to displacement [Fig. 1(b)]. The width of the peak, which is inversely proportional to the reflectivity, determines the sensitivity of the structure.

To achieve high sensitivity in Fabry-Perot cavity sensor structures, therefore, requires either the use of highly reflecting mirrors or a long propagation distance. Exceedingly high sensitivity, for example, can be achieved when the distance between the mirrors is macroscopic. However, when the distance between the mirrors is comparable to the wavelength, maintaining high sensitivity becomes more challenging as the requirement for high reflectivity becomes more stringent. At the same time, the reflectivity of a nanoscale mirror becomes more sensitive to fabrication-related disorder.[7] Moreover, a Fabry-Perot sensor no longer functions when the distance between the mirrors is much smaller than the wavelength, since no resonance is supported at that length scale. On the other hand, sensing distance change in the re-

gime where the distance itself is in the nanoscale could be potentially important for applications such as biosensing and atomic force microscopy.[8]

Here, we propose an alternative sensing mechanism based upon photon tunneling and Fano interference. We show that by coupling two photonic crystal slabs together, and by choosing the spacing between the slabs to be far smaller than the wavelength, one can construct a sensor, for which the transmission is sensitively dependent upon the distance between the slabs. Unlike the standard Fabry-Perot sensors,[1–6,9] in which photons propagate between the mirrors, here the photons can in addition tunnel between them. This mechanism, therefore, no longer requires the long propagation distance or high reflectivity to achieve high sensitivity. The sensing mechanism rather exploits the presence of guided resonance in each slab and the near-field coupling
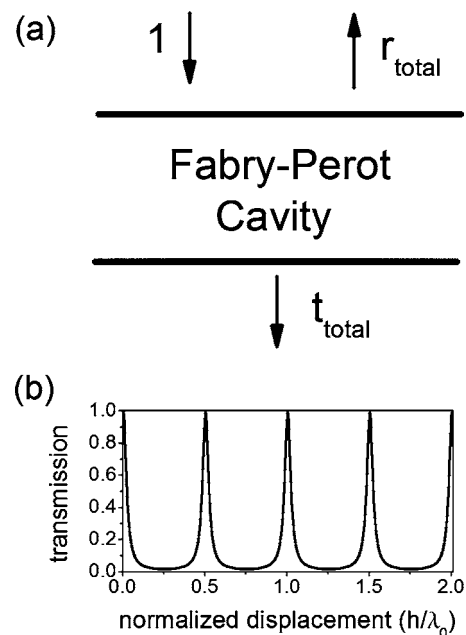

FIG. 1. (a) Schematic of a Fabry-Perot cavity structure. (b) Transmission through a Fabry-Perot cavity structure as a function of displacement normalized by the operation wavelength λ_0. The reflectivity of each mirror is 0.87.

[a] Electronic mail:wjsuh@standford.edu
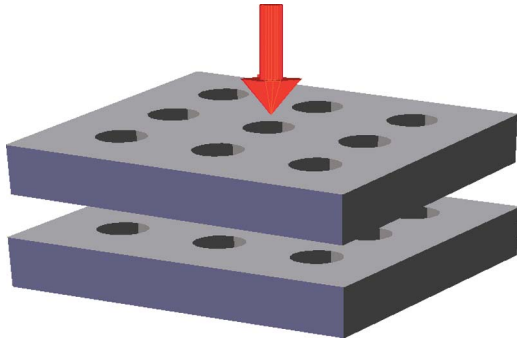
98, 033102-1

FIG. 2. (Color) A coupled photonic crystal slab structure. The arrow represents the direction of the externally incident light.

between the resonances. For a gap size as small as 250 nm, the displacement sensitivity can still reach below the nanometer regime.

II. ANALYSIS OF THE NEAR-FIELD SENSOR STRUCTURE

We consider a structure that consists of two photonic crystal slabs as shown in Fig. 2. Each slab consists of a periodic array of air holes in a high-index guiding layer. Such slab supports guided resonances,[10–14] which are strongly confined in the slab and yet can couple to free space radiation through coherent Bragg scattering. By placing two slabs in close proximity to each other such that the optical near field of the resonances overlap, the guided resonances in the two slabs can couple through an evanescent tunneling pathway in addition to the free space propagation pathway between the slabs. In such near-field regime, the sensing characteristic is completely different from the standard Fabry-Perot cavities, since the variation of the displacement influences both the near-field and the far-field coupling between the guided resonances.

As a concrete example, we consider photonic crystal slabs with dielectric constant of 12, which corresponds to Si at optical frequencies. The slab has a thickness of $0.1a$, where a is the lattice constant, and the air holes have a radius of $0.2a$ [Fig. 3(a)]. The transmission through one slab, calculated by finite-difference time-domain (FDTD)[15] simulations, is shown in Fig. 3(b). In the vicinity of frequency $\omega = 0.54(c/a)$, the transmission exhibits a Fano line shape indicating the existence of a guide resonance. When we plot the power density of the magnetic field in the photonic crystal slab structure, we indeed see the presence of the guided resonance mode shown in Fig. 3(c). From the field distribution, we can see that the guided resonance mode shows an exponentially decay along the propagation direction of the incident light.

Previously, a displacement sensor exploiting the high reflectivity of the slabs has been proposed.[9,16] Here, we intentionally choose a frequency of $\omega = 0.519(c/a)$, at which the intensity reflectivity of each slab is only 0.76, to demonstrate a different sensing mechanism. At this frequency, the transmission response for the coupled slab structure is shown as a function of the displacement in Fig. 4. When the displacement is $h = 0.51\lambda_0$, where $\lambda_0 = 1.927a$ is the operation wave-
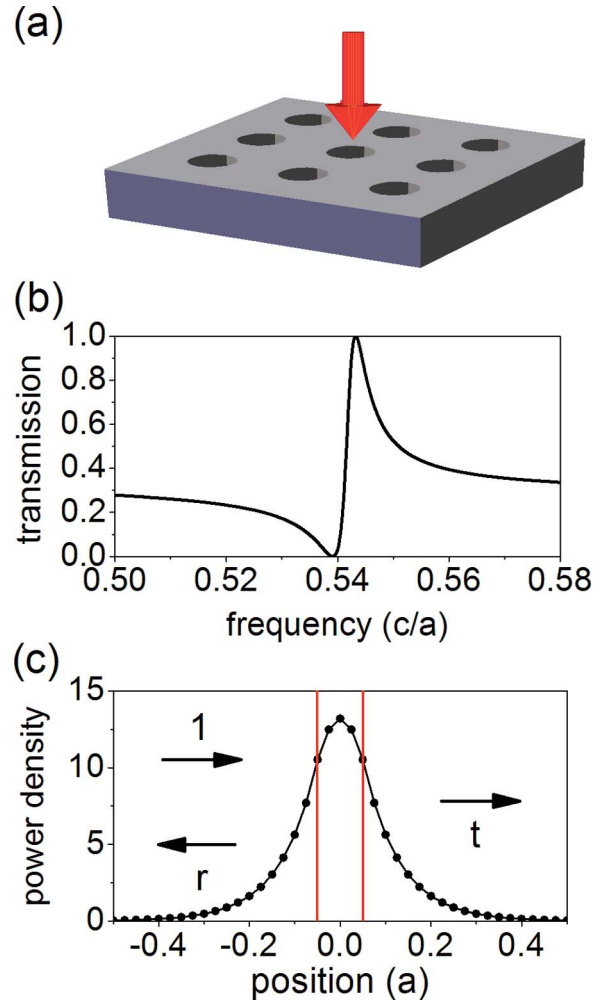

FIG. 3. (Color) (a) A photonic crystal slab structure. The arrow represents the direction of the externally incident light. (b) Transmission spectrum of a single-photonic crystal slab with thickness of $0.1a$, where a is the lattice constant, and air holes of radius $0.2a$. The dielectric constant of the slab is 12. (c) Magnetic power density of the guided resonance mode inside a photonic crystal slab with thickness of $0.1a$, where a is the lattice constant, and air holes of radius $0.2a$. The red line indicates the location of the photonic crystal slab along the propagation direction and the black line represents the power density of the guided resonance mode upon normally incident light, at frequency $\omega = 0.54(c/a)$, in arbitrary units.

length in air when $\omega = 0.519(c/a)$, the evanescent coupling between the photonic crystal slabs is negligible and therefore the transmission through the coupled slab structure shows a resonance with a symmetric Lorentzian line shape with re-
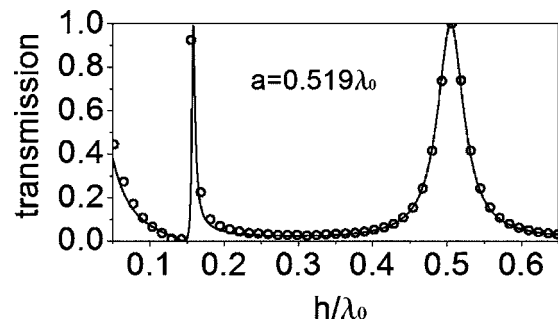

FIG. 4. Transmission as a function of normalized displacement through a two-slab structure, at a fixed frequency $0.519(c/a)$. Each slab has a transmission spectrum as in Fig. 3(b). The solid line is from coupled-mode theory and the open circles represent the FDTD simulations.
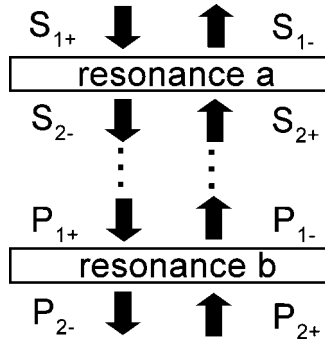
FIG. 5. Schematic of a theoretical model of two resonators, each coupling with incoming and outgoing waves as indicated by the arrows.

spect to the displacement. Notice, however, an additional peak where the displacement is $h=0.16\lambda_0$. The line shape of the peak is non-Lorentzian, and such line shape cannot be accomplished with far-field coupling alone.

To account for the simulation results, we develop a theoretical model using the temporal coupled-mode theory for optical resonators. The model, schematically shown in Fig. 5, consists of two optical resonances with amplitudes A and B. Assuming both resonances to be even with respect to the mirror plane parallel to the slabs, the dynamic equation for the amplitude A is:[17]

$$\frac{dA}{dt} = (j\omega_0 - \gamma)A + \alpha S_{1+} + \alpha S_{2+} + j\kappa B, \qquad (2)$$

$$S_{1-} = r_d S_{1+} + t_d S_{2+} + \alpha A, \quad S_{2-} = t_d S_{1+} + r_d S_{2+} + \alpha A, \quad (3)$$

where ω_0 and γ are the frequency and the decay rate of the resonance, respectively. S_{1+}, S_{2+}, S_{1-}, and S_{2-} are the incoming and outgoing waves from either side of the slab, and t_d and r_d are the background transmission and reflection coefficients of the slab. The coupling coefficient κ describes the evanescent tunneling rate between resonance A and B, and is real due to energy conservation and mirror symmetry constraints. $\alpha=\sqrt{-\gamma(r_d+t_d)}$ is the coupling coefficient that describes the strength of coupling between the propagating waves and the resonance.[18] Similarly, the equations for the amplitude B in the second resonance are

$$\frac{dB}{dt} = (j\omega_0 - \gamma)B + \alpha P_{1+} + \alpha P_{2+} + j\kappa A, \qquad (4)$$

$$P_{1-} = r_d P_{1+} + t_d P_{2+} + \alpha B, \quad P_{2-} = t_d P_{1+} + r_d P_{2+} + \alpha B, \qquad (5)$$

where P_{1+}, P_{2+}, P_{1-}, and P_{2-} are the incoming or outgoing waves at either side of the second slab. Since the wave propagates between the slabs, we have

$$P_{1+} = \exp(-j\phi)S_{2-}, \quad P_{1-} = \exp(j\phi)S_{2+}, \qquad (6)$$

where $\phi=(\omega/c)h$, and h is the distance between the edges of the slabs. From Eqs. (2)–(6), the total transmission through the coupled slab structure can be determined as

$$t_{\text{total}} = \frac{j\kappa\alpha^2[e^{j2\phi} - (r_d - t_d)^2] + e^{j\phi}\{\alpha^2 + t_d[\gamma + j(\omega - \omega_0 + \kappa)]\}\{\alpha^2 + t_d[\gamma + j(\omega - \omega_0 - \kappa)]\}}{\alpha^4 + 2j\alpha^2[\kappa e^{j\phi} + r_d(-j\gamma + \omega - \omega_0)] - (e^{j2\phi} - r_d^2)\{\kappa^2 + [\gamma + j(\omega - \omega_0)]^2\}}. \qquad (7)$$

In Eq. (7), the amplitude of the coupling constant κ, which represents the near-field coupling strength, depends on the displacement h exponentially. For the simulated structure, we have numerically determined the coupling constant to be $\kappa=-0.19e^{-h/(0.145a)}$ by fitting the displacement dependency of the transmission coefficient at $\omega=0.519(c/a)$. The decay length (0.145a) here is consistent with a rough estimate. Since the mode is a first-order resonance, the corresponding guided mode has $k_\parallel=2\pi/a$, where $k_\parallel$ is the in-plane wave vector, and hence the decay length is approximately $1/a\sqrt{k_\parallel^2-(\frac{\omega}{c})^2}=0.166$. With the coupling constant as determined above, we calculate using Eq. (7) the transmission coefficients as a function of both the displacement and the frequencies, and compare that with FDTD simulations (Fig. 6). The two show excellent agreement indicating that the first-order perturbative formalism in the coupled photonic crystal slab structure is valid. Notice, in particular, the existence of high displacement-sensitivity region over a relatively wide frequency range between $0.5(c/a)$ and $0.54(c/a)$. High displacement sensitivity can therefore be achieved without the need for accurate control over the source fre-

quency, which is not possible in conventional high-sensitivity optical displacement sensors that are based on Fabry-Perot interferometers, ring-resonators, microspheres, or other high-Q resonators.

In the structure simulated above, with a mirror reflectivity of 76%, a 20-dB transmission contrast can be obtained when the distance between the slabs varies by only $0.02a$. In comparison, to accomplish the same sensitivity with a Fabry-Perot structure requires a mirror with reflectance exceeding 0.987. In addition, the structure does not require high quality-factor guided resonances: The quality factor of the resonance in each slab is less than 150. Similar quality factors have been experimentally observed in photonic crystal slab structures.[16] The use of low quality factor resonance and low reflectivity mirrors generally results in structures that are robust against fabrication-related disorders.[9]

III. FINAL REMARKS

As closing remarks, we note that the displacement sensitivity can be further enhanced by using a guided resonance mode with a shorter spatial decay length. This can be done
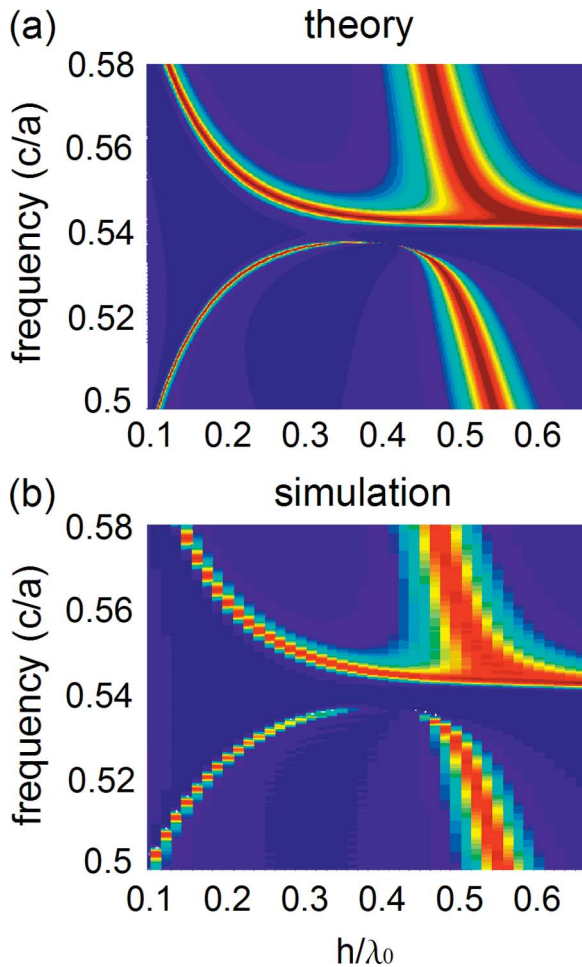
FIG. 6. (Color) Transmission through the two-slab structure as shown in Fig. 2(a), as a function of displacement and frequency. The displacement between the two slabs is normalized to the wavelength of the incident light $\lambda_0 = 1.927a$. Blue and red correspond to 0% and 100% transmission, respectively. (a) Coupled-mode theory simulation using Eq. (7). The direct coupling coefficient is $\kappa = -0.19e^{-h/(0.145a)}$. (b) FDTD results.

by using a higher-order guided resonance mode, or by using a slab with a larger thickness, which possesses guided resonance modes with lower normalized frequencies with respect to the lattice constant. Also, in our design, the edge-to-edge displacement between the slabs is approximately 250 nm when the wavelength of the incident light is 1550 nm. Such distance for an air gap is compatible with the micro-electro-mechanical systems technology.[19] In conclusion, the evanescent coupling of guided resonance in photonic crystal structures with strong index contrast provides a tool for optical engineering on the nanoscale.

ACKNOWLEDGMENTS

[1]C. E. Lee and H. F. Taylor, J. Lightwave Technol. **9**, 129 (1991).
[2]Y. Kim and D. P. Neikirk, IEEE Photonics Technol. Lett. **7**, 1471 (1995).
[3]J. Han, D. P. Neikirk, M. Clevenger, and J. T. McDevitt, Proc. SPIE **2881**, 171 (1996).
[4]J. Zhou, S. Dasgupta, H. Kobayashi, J. M. Wolff, H. E. Jackson, and J. T. Boyd, Opt. Eng. (Bellingham) **40**, 598 (2001).
[5]W. J. Wang, R. M. Lin, Y. Ren, T. T. Sun, and D. G. Guo, Microwave Opt. Technol. Lett. **39**, 240 (2003).
[6]C. J. Lin and F. G. Tseng, Sens. Actuators, A **114**, 163 (2004).
[7]O. Kilic, S. Kim, W. Suh, Y. A. Peter, A. S. Sudbo, M. F. Yanik, S. Fan, and O. Solgaard, Opt. Lett. **29**, 2782 (2004).
[8]B. E. N. Keeler, D. W. Carr, J. P. Sullivan, T. A. Friedmann, and J. R. Wendt, Opt. Lett. **29**, 1182 (2004).
[9]W. Suh, M. F. Yanik, O. Solgaard, and S. Fan, Appl. Phys. Lett. **82**, 1999 (2003).
[10]S. Fan and J. D. Joannopoulos, Phys. Rev. B **65**, 235112 (2002).
[11]A. Erchak, D. J. Ripin, S. Fan, P. Rakich, J. D. Joannopoulos, E. P. Ippen, G. S. Petrich, and L. A. Kolodziejski, Appl. Phys. Lett. **78**, 563 (2001).
[12]H. Y. Ryu, Y. H. Lee, R. L. Sellin, and D. Bimberg, Appl. Phys. Lett. **79**, 3573 (2001).
[13]S. S. Wang, R. Magnuson, J.S. Bagby, and M.G. Moharam, J. Opt. Soc. Am. A **7**, 1470 (1990).
[14]S. Noda, M. Yokoyama, M. Imada, A. Chutinan, and M. Mochizuki, Science **293**, 1123 (2000).
[15]K.S. Kunz and R.J. Luebbers, *The Finite-Difference Time-Domain Methods for Electromagnetics* (CRC, Boca Raton, 1993); A. Taflove and S. Hagness, *Computational Electrodynamics: The Finite-Difference Time-Domain Methods* (Artech House, Boston, 2000).
[16]V. Lousse, W. Suh, O. Kilic, S. Kim, O. Solgaard, and S. Fan, Opt. Express **12**, 1575 (2004).
[17]H. A. Haus, *Waves and Fields in Optoelectronics* (Prentice Hall, Englewood Cliffs, 1984).
[18]S. Fan, W. Suh, and J. D. Joannopoulos, J. Opt. Soc. Am. A **20**, 569 (2003).
[19]M. Datta, M. W. Pruessner, D. P. Kelly, and R. Ghodssi, Solid-State Electron. **48**, 1959 (2004).